BRIEF REPORTS

Brief Reports are accounts of completed research which do not warrant regular articles or the priority handling given to Rapid Communications; however, the same standards of scientific quality apply. (Addenda are included in Brief Reports.) A Brief Report may be no longer than four printed pages and must be accompanied by an abstract. The same publication schedule as for regular articles is followed, and page proofs are sent to authors.

Bifurcation and chaos induced by a time-periodic vector potential

Suhan Ree and L.E. Reichl
Center for Studies in Statistical Mechanics and Complex Systems, The University of Texas at Austin, Austin, Texas 78712
(Received 5 May 1995; revised manuscript received 14 July 1995)

The behavior of a classical charged particle moving between two coaxial infinitely long cylinders is studied. The inner cylinder is a tightly wound solenoid with a small radius carrying an oscillating current with frequency ω_0. The outer cylinder carries no current and is formed by a thin dielectric material. We study the regime $\omega_0/c \ll 1/b$, where b is the radius of the outer cylinder. We find that for low enough ω_0 there is no chaos in the phase space of the particle. However, the emergence of resonances and chaos can be observed as ω_0 is increased above a threshold value. Also, chaos in the phase space is observed as the magnitude of current is increased.

PACS number(s): 05.45.+b, 41.20.Bt

I. INTRODUCTION

There are few examples of measurable conservative systems in which primary nonlinear resonances and chaos suddenly appear in the phase space as certain controllable parameters of the system are varied. In this Brief Report we shall show that it can happen to a classical particle confined to a cylindrical box and driven by a time-periodic electromagnetic vector potential. We will examine the motion of a classical particle of mass m and charge q moving in the region outside a tightly wound solenoid with radius a carrying a monochromatic alternating current of the form $\mathbf{J}(\mathbf{r},t) = J_0\,\delta(r-a)\cos(\omega_0 t)\,\hat{\phi}$. [We use cylindrical coordinates (r,ϕ,z), where the z axis coincides with the solenoid axis.] There is an outer cylinder with radius b made of a thin dielectric material which confines the particle. The region inside the solenoid is empty space, as are the regions between the cylinders and outside the cylinders. The particle, which moves in the space between the solenoid and the outer cylinder (the region $a < r < b$), behaves as if the two walls are infinitely hard. Because of the oscillating current on the solenoid, there will be time varying electric and magnetic fields in all three regions. The electromagnetic field does not behave as if the walls are hard. At $r = a$ there is a surface current. At $r = b$ there is an extremely thin dielectric. The magnetic field will be discontinuous across the wall at $r = a$, but will be continuous across the wall at $r = b$. In fact, we can assume the wall at $r = b$ does not exist as far as the electromagnetic field is concerned. It does exist for the particle.

We will assume that there are no free charges, except for the particle. Therefore, the scalar potential is identically zero everywhere, but there will be a vector potential $\mathbf{A}(\mathbf{r},t) = A_\phi(r,t)\hat{\phi}$. From Maxwell's equations the vector potential satisfies

$$\frac{\partial}{\partial r}\left(\frac{1}{r}\frac{\partial}{\partial r}(rA_\phi)\right) = \epsilon_0\mu_0\frac{\partial^2}{\partial t^2}A_\phi - \mu_0 J_0\,\delta(r-a)\cos(\omega_0 t), \tag{1}$$

where ϵ_0 is the permittivity, μ_0 is the permeability, and $A_r = A_z = 0$ [1]. In the region, $a < r < b$, Eq. (1) has the solution

$$\mathbf{A}(r,t) = \frac{\mu_0 J_0}{k}\frac{J_1(kr_<)[N_1(kr_>)\cos(\omega_0 t) - J_1(kr_>)\sin(\omega_0 t)]}{J_0(ka)N_1(ka) - J_1(ka)N_0(ka)}\,\hat{\phi}, \tag{2}$$

where $r_>$ ($r_<$) is the larger (smaller) of r and a, $k = \omega_0/c$, and J_ν and N_ν are Bessel functions of order ν. If the frequency of the oscillating current is low enough ($kb \ll 1$), the vector potential in the region between the two walls is given by $\mathbf{A}(r,t) \simeq \frac{\alpha_0}{r}\cos(\omega_0 t)\,\hat{\phi}$, where $\alpha_0 = \mu_0 J_0 a^2/2$. As a result, for low frequencies the electric field is $\mathbf{E} = -\frac{\partial \mathbf{A}}{\partial t} = \frac{\alpha_0\omega_0}{r}\sin(\omega_0 t)\,\hat{\phi}$ and the magnetic field $\mathbf{B} = \nabla\times\mathbf{A} = 0$ in the region between the two walls.

With this vector potential, the Hamiltonian for the particle between the two walls takes the form

$$H(t) = \frac{p_r^2}{2m} + \frac{[p_\phi - q\alpha_0\cos(\omega_0 t)]^2}{2mr^2} + \frac{p_z^2}{2m} + V_a(r) + V_b(r). \tag{3}$$

 ©1996 The American Physical Society

V_a and V_b are the potentials associated with the infinitely hard walls at $r = a$ and $r = b$ ($V_a = 0$ for $r > a$ and $V_a = \infty$ for $r < a$, and $V_b = 0$ for $r < b$ and $V_b = \infty$ for $r > b$). The Hamiltonian is most conveniently written in cylindrical coordinates. It depends only on the the radius and not on the azimuthal angle ϕ, or on z. Therefore p_z and p_ϕ are constants of the motion. Without loss of generality, we can let $p_z = 0$ and $p_\phi = l_\phi > 0$. We now divide the Hamiltonian into two parts, $H(t) = H_0 + H_1(t)$, where H_0 is a time-independent part,

$$H_0 = \frac{p_r^2}{2m} + \frac{L^2}{2mr^2} + V_a(r) + V_b(r), \tag{4}$$

with $L^2 \equiv l_\phi^2 + q^2\alpha_0^2/2$ (assume $L > 0$), and $H_1(t)$ is a time-periodic part,

$$H_1(t) = -\frac{q l_\phi \alpha_0 \cos(\omega_0 t)}{mr^2} + \frac{q^2\alpha_0^2 \cos(2\omega_0 t)}{4mr^2}. \tag{5}$$

Before we examine the behavior of this system it is useful to rewrite the full Hamiltonian $H(t)$ in terms of the action angle variables of the time-independent Hamiltonian H_0.

In Sec. II, we obtain the action-angle variables for the system whose dynamics is governed by H_0 and we determine the natural frequencies of the system, $\omega = \frac{\partial H_0}{\partial J}$. In Sec. III, we use the full Hamiltonian to determine the resonance conditions, and from numerical results we observe emergence, bifurcation, and overlap of primary resonances by varying ω_0 and $q\alpha_0$. Finally, in Sec. IV, we make some concluding remarks.

II. TIME-INDEPENDENT HAMILTONIAN H_0

In this section we consider the case when the motion is governed by the time-independent Hamiltonian H_0 [cf. Eq. (4)]. We shall restrict ourselves to an inner radius a small enough that the particle never hits the inner wall. This will be the case if the angular momentum is such that $L > a\sqrt{2mE_0}$. The particle will bounce between the outer wall, $r = b$, and an inner turning point, $r_0 = \frac{L}{\sqrt{2mE_0}}$ (the point where $p_r = 0$). Between collisions with the walls, the motion of the particle is governed by Hamiltonian equations, $\frac{dp_r}{dt} = -\frac{\partial H_0}{\partial r} = \frac{L^2}{mr^3}$ and $\frac{dr}{dt} = \frac{\partial H_0}{\partial p_r} = \frac{p_r}{m}$. These may be integrated [for initial conditions, $r(0) = r_0$ and $p(0) = 0$] to give

$$r(t) = \sqrt{\frac{2E_0}{m}}\sqrt{\frac{L^2}{4E_0^2} + t^2} \quad \text{for} \quad -\frac{T}{2} \le t \le \frac{T}{2}, \tag{6}$$

where $T = \frac{1}{E_0}\sqrt{2mE_0b^2 - L^2}$ is the period of the motion. The momentum is given by

$$p_r(t) = \frac{\sqrt{2mE_0}\, t}{\sqrt{\frac{L^2}{4E_0^2} + t^2}} \quad \text{for} \quad -\frac{T}{2} \le t \le \frac{T}{2}. \tag{7}$$

It is useful to obtain a canonical transformation to action-angle variables for the radial coordinates

$$J = \frac{1}{2\pi}\oint p_r dr = \frac{\sqrt{2mE_0}}{\pi}\left[\sqrt{b^2 - r_0^2} - r_0 \cos^{-1}\left(\frac{r_0}{b}\right)\right]. \tag{8}$$

The angle variable satisfies the equation

$$\dot{\theta} = \frac{\partial E_0}{\partial J} = \frac{2\pi E_0}{\sqrt{2mb^2E_0 - L^2}}, \tag{9}$$

where $\omega \equiv \dot{\theta} = 2\pi/T$ is the natural frequency of the motion. Note that the frequency ω has a minimum value given by $\omega_{min} = \frac{2\pi L}{mb^2}$ for $E_0 = \frac{L^2}{mb^2}$. Since all quantities in the expression for ω are constants of the motion (for dynamics governed by H_0), the angle at time t is simply $\theta(t) = \omega t$ [with the convention that $\theta(0) = 0$ at the turning point]. In Fig. 1, we plot the frequency ω as a function of energy E_0 for $m = 1$, $L = 1$, and $b = 10$. For these parameters, the minimum frequency occurs at $\omega = \omega_{min} = \frac{\pi}{50}$ for energy $E_0 = 0.01$. This corresponds to the longest period orbit allowed by the system for these parameter values.

Since the frequency has a minimum value, we find that there are two possible energies, and therefore two possible trajectories, for each frequency. It will prove useful to write the energy in terms of the minimum frequency ω_{min}. If we let $\omega = x\omega_{min}$, then we find

$$E_\pm = \frac{x^2L^2}{mb^2}\left[1 \pm \sqrt{1 - \frac{1}{x^2}}\right]. \tag{10}$$

The inner turning point of an orbit with energy E_0 is $r_0 = L/\sqrt{2mE_0}$. Therefore, the positions of the inner turning points for orbits of energy E_+ or E_- are given by

$$r_0^\pm = \frac{L}{\sqrt{2mE_\pm}} = \frac{b}{\sqrt{2x}}\left[1 \pm \sqrt{1 - \frac{1}{x^2}}\right]^{-1/2}. \tag{11}$$

The canonical transformation from radial variables (p_r, r) to action-angle variables (J, θ) is given by

$$r(J,\theta) = \frac{1}{\pi}\sqrt{\frac{\pi^2L^2 + \theta^2(2mb^2E_0 - L^2)}{2mE_0}} \tag{12}$$

and

$$p_r(J,\theta) = \frac{\theta}{\pi}\sqrt{\frac{(2mE_0)(2mb^2E_0 - L^2)}{L^2 + \frac{\theta^2}{\pi^2}(2mb^2E_0 - L^2)}} \tag{13}$$

for $-\pi \le \theta \le \pi$.

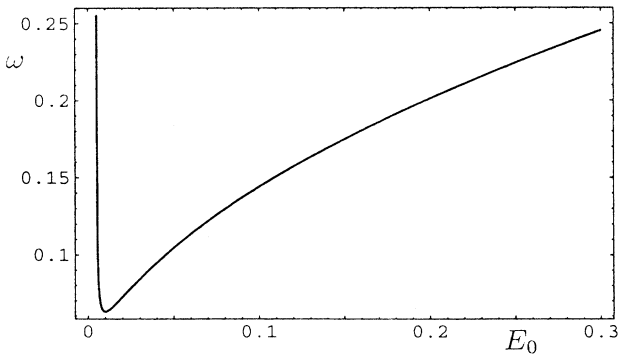

FIG. 1. Frequency $\omega = 2\pi E_0/\sqrt{2mb^2E_0 - L^2}$ versus E_0 for $m = 1$, $b = 10$, and $L = 1$. The minimum frequency $\omega_{min} = \pi/50$ occurs at $E_0 = 0.01$.

III. FULL DYNAMICS

Let us now write the full Hamiltonian $H(t)$ in terms of action-angle variables for the time-independent system H_0. It takes the form

$$H(t) = E_0(J) - \frac{q l_\phi \alpha_0}{m r^2}\cos(\omega_0 t) + \frac{q^2\alpha_0^2}{4mr^2}\cos(2\omega_0 t). \quad (14)$$

The quantities $r^{-2}(J,\theta)$ are even periodic functions of the angle θ. Therefore we can expand them in a Fourier cosine series. If we do this, then Eq. (14) can be written in the form

$$H(t) = E_0(J) - \frac{q l_\phi \alpha_0}{2m}\sum_{n=-\infty}^{\infty} b_n(J)\cos(n\theta - \omega_0 t) + \frac{q^2\alpha_0^2}{8m}\sum_{l=-\infty}^{\infty} b_l(J)\cos(l\theta - 2\omega_0 t), \quad (15)$$

where $b_n = \frac{2mE_0}{\pi}\int_{-\pi}^{\pi} \frac{d\theta\,\cos(n\theta)}{[L^2 + \frac{\theta^2}{\pi^2}(2mb^2E_0 - L^2)]}$.

The two sets of traveling cosine waves in Eq. (15) give rise to infinite sets of "primary" nonlinear resonance zones in the phase space of the system [2]. A "primary" resonance (as opposed to a fractional resonance) occurs when the frequency ω_0 of the vector potential is equal to an integer multiple of the natural frequency ω. The cosine waves which are proportional to α_0 give rise to resonance zones which dominate the phase space for small $q\alpha_0$, while those proportional to α_0^2 give rise to resonance zones which dominate the phase space for large $q\alpha_0$. We will write the resonance conditions for the two sets separately.

A. "α_0" resonances

The resonance condition is $\omega_0 = n\omega(J_n^r)$ or

$$\frac{\omega_0}{n} = \frac{2\pi E_0(J_n^r)}{\sqrt{2mb^2E_0(J_n^r) - L^2}}, \quad (16)$$

where J_n^r locates the position of the nth resonance zone in the (J,θ) phase space. When $\omega_0 < \omega_{min}$, no primary resonance of the "α_0" type can occur.

B. "α_0^2" resonances

The resonance condition is $2\omega_0 = l\omega(J_n^r)$ or

$$\frac{2\omega_0}{l} = \frac{2\pi E_0(J_l^r)}{\sqrt{2mb^2E_0(J_l^r) - L^2}}, \quad (17)$$

where J_l^r locates the position of the lth resonance zone in the (J,θ) phase space. No "α_0^2" primary resonances can occur if $\omega_0 < \omega_{min}/2$.

We can now use the resonance conditions in Eqs. (16) and (17) to locate the resonance zones in phase space when $q\alpha_0$ is small. Approximate values of the energies of trajectories in the region of resonances are given by Eq. (10). An "α_0" resonance occurs when the external field frequency $\omega_0 = n\omega$ or $x = \frac{\omega_0}{n\omega_{min}}$. An "$\alpha_0^2$" resonance is given by the condition that $\omega_0 = \frac{1}{2}l\omega$ or $x = \frac{2\omega_0}{\omega_{min}}$. We can use Eq. (11) to locate the region in phase space where we expect to find a resonance.

Let us now examine how the resonances emerge in the phase space and bifurcate when the external field frequency has values $\omega_0 \approx \frac{1}{2}\omega_{min}$. In Fig. 2, we show the behavior of the phase space in this region of external field frequency by gradually changing ω_0 near $\omega_{min}/2$. In Fig. 2, we use $l_\phi = 1$, $m = 1$, $b = 10$ ($\omega_{min} \simeq \frac{\pi}{50}$), and $q\alpha_0 = \frac{5}{20\pi}$. Because of the small value of $q\alpha_0$, we expect the resonance conditions in Eqs. (16) and (17) to give good predictions. The lowest external field frequency at which a resonance can be induced in the system is $\omega_{min}/2 \simeq 0.01\pi$. This is an "$\alpha_0^2$" resonance. We define the threshold frequency ω_{th} as 0.01π. In Fig. 2 we show a sequence of plots, with ω_0 ranging from $0.9950\,\omega_{th}$ to $1.053\,\omega_{th}$, which shows the emergence and bifurcation of the first "α_0^2" primary resonance. In Fig. 2(a), $\omega_0 = 0.9950\,\omega_{th}$ and no resonance exists. In Fig. 2(b), $\omega_0 = \omega_{th}$ and a single resonance has emerged. (A similar phenomenon was observed in [3].) In Figs. 2(c) and 2(d), the bifurcation process starts to become visible. In Fig. 2(e) the original single resonance has split into two distinct resonances. The resonance that has its island on the left has its unstable fixed point at $r = 10$ (the surface of the outer cylinder). On the other hand, the resonance on the right has its stable fixed point at $r = 10$ and $p_r \simeq \pm 0.7$. As we increase ω_0 further, the resonances continue to move apart.

In Fig. 3, we show the case $\omega_0 = \frac{2\pi}{75} \simeq \frac{4}{3}\omega_{min}$. For this case we have both "α_0^2" and "α_0" first primary resonances. They can be located with the help of Eq. (11). The "α_0^2" first primaries are located at $x = \frac{8}{3}$ or $r_0^+ = 1.910$ and $r_0^- = 9.816$. The "α_0" first primaries are

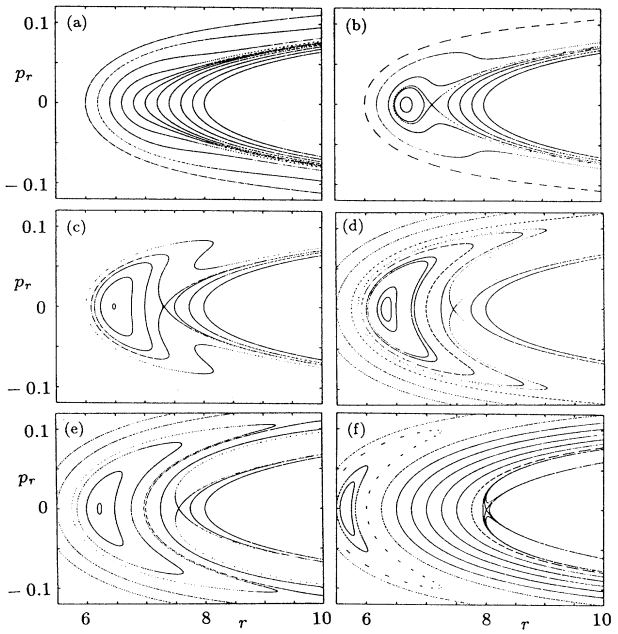

FIG. 2. Strobe plots of the (p_r, r) phase space for $m = 1$, $l_\phi = 1$, $b = 10$, $q\alpha_0 = \frac{5}{20\pi}$ ($\omega_{min}/2 \simeq 0.01\pi \equiv \omega_{th}$), and (a) $\omega_0 = 0.9950\,\omega_{th}$, (b) $\omega_0 = \omega_{th}$, (c) $\omega_0 = 1.005\,\omega_{th}$, (d) $\omega_0 = 1.010\,\omega_{th}$, (e) $\omega_0 = 1.020\,\omega_{th}$, and (f) $\omega_0 = 1.053\,\omega_{th}$.

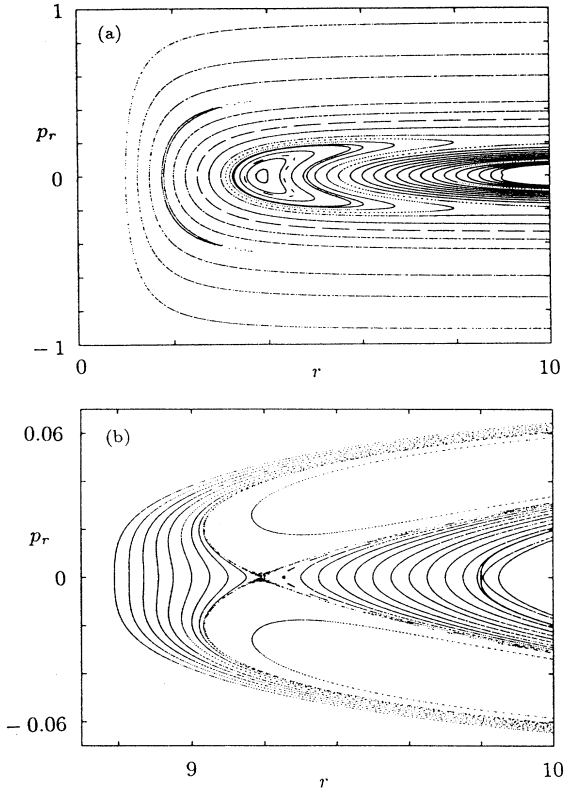

FIG. 3. Strobe plots of the (p_r, r) phase space for $m = 1$, $l_\phi = 1$, $b = 10$, $q\alpha_0 = \frac{5}{20\pi}$, and $\omega_0 = \frac{2\pi}{75} \simeq \frac{4}{3}\,\omega_{min}$. (a) Large scale view. (b) Magnification of the region $8.7 \leq r \leq 10$.

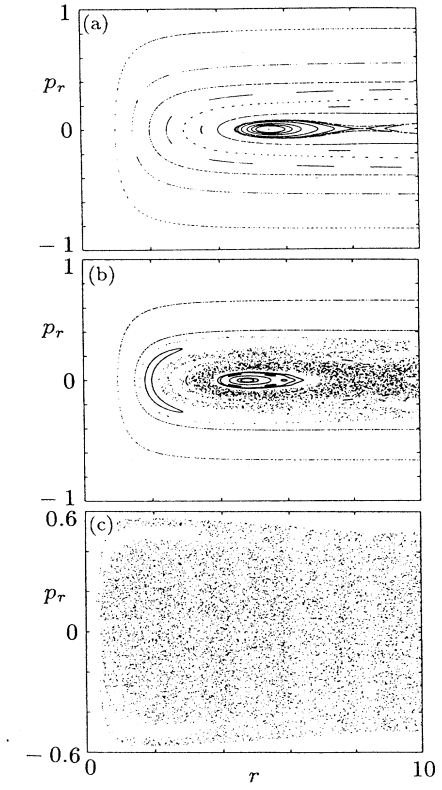

FIG. 4. Strobe plot of the (p_r, r) phase space for $m = 1$, $l_\phi = 1$, $b = 10$, and $\omega_0 = \frac{\pi}{50} \simeq \omega_{min}$. (a) $q\alpha_0 = \frac{10}{20\pi}$, (b) $q\alpha_0 = \frac{20}{20\pi}$, and (c) $q\alpha_0 = \frac{50}{20\pi}$.

located at $x = \frac{4}{3}$ or $r_0^+ = 4.114$ and $r_0^- = 9.114$.

It is also interesting to examine the phase space for increasing values of the external field amplitude $q\alpha_0$, where the predictions given by the resonance conditions Eqs. (16) and (17) break down since they neglect terms of order $q\alpha_0$ and $q^2\alpha_0^2$. In Fig. 4, we show the phase space for $\omega_0 = \frac{\pi}{50} \simeq \omega_{min}$ and $q\alpha_0 = \frac{10}{20\pi}$, $\frac{20}{20\pi}$, $\frac{50}{20\pi}$. We see the emergence of global chaos with increasing strength of the solenoid current.

IV. DISCUSSION

In this Brief Report, we have observed the creation and the emergence of a primary resonance when the frequency ω_0 of the electromagnetic vector potential reaches the value $\omega_{min}/2$. An interesting bifurcation pattern emerges as we increase ω_0. We have also observed the overlap of resonant zones and the onset of chaos as the magnitude of the current (represented by $q\alpha_0$) was increased.

In the discussion above, we set the radius of the inner cylinder to the value $a = 0.1$, which is very small compared to the radius of the outer cylinder, $b = 10$. When a is larger, the inner cylinder should be taken into account even with small $q\alpha_0$. But we can expect to obtain similar results by the same method of analysis.

ACKNOWLEDGMENTS

The authors wish to thank the Welch Foundation, Grant No. 1052 for partial support of this work, and the University of Texas High Performance Computing Center for the use of its facilities.

[1] J.D. Jackson, *Classical Electrodynamics* (John Wiley & Sons, New York, 1975).

[2] L.E. Reichl, *The Transition to Chaos In Conservative Classical Systems: Quantum Manifestations* (Springer-Verlag, New York, 1992).

[3] G.H. Walker and J. Ford, Phys. Rev. **188**, 416 (1969).